Laser Trapping of Micrometer-Sized Objects

Kathryn Child
Philip I. Thomas
Department of Physics
Washington University in St. Louis
6 December 2012

Abstract

We characterized the motion of micrometer-scale beads and blood cells undergoing Brownian motion and under trapping by an optical tweezer apparatus. Diffusion coefficients and Boltzmann's constant were calculated based upon variations in the bead and cell movements.

Introduction and Background

Brownian Motion

Brownian motion describes the random movement of small particles. The phenomenon is named for biologist Robert Brown[i], who is credited with first describing the phenomena while observing the random motion of pollen in solution. In addition to small particles in solution, models for Brownian motion suitably describe numerous other processes, ranging from molecular movement to stock market prices.

Numerous mathematical models for Brownian motion exist, mainly in the field of particle theory. Classical mechanics fails to adequately describe the high number of interactions between multiple particles. Thus, most modern models take a thermodynamics-based, statistical approach to quantification of multiparticle systems. This is rooted in the Second Law of Thermodynamics [ii], which describes the increasing entropy of a closed system.

When analyzing one particle, Brownian motion is suitably modeled as a random walk. Random walks originate in term as the seemingly random mix of forward and backward steps by a drunk. The term was coined in 1905 by Karl Pearson to describe random motion in discrete steps of a fixed length [iii]. These discrete steps form a binomial distribution that may be approximated as a continuous normal distribution as the number of steps increases[iv]. Thus, when analyzing a single particle undergoing Brownian motion, its displacement may be modeled as a Gaussian distribution.

Diffusion

Diffusion is a random process modeled as a series of differential equations called Ficks Equations.[v]

A diffusion coefficient for two-dimensional motion may be calculated as a function of the statistical average of the displacement in each dimension, as shown in **Equation 1**.

$D=\langle \Delta x^2+\Delta y^2 \rangle/(4\Delta t)$ (Equation 1)

Boltzmann Constant

The Boltzmann Constant is named for Ludwig Boltzmann, an Austrian physicist who made important contributions to kinetic theory. The number originates from gas theory, where the constant was first quantified as the gas constant divided by Avogadro's number. However, the constant is fundamental in statistical mechanics for relating entropy to the number of microstates.

Thus, the Boltzmann Constant is important when describing Brownian motion because it bridges the second law of thermodynamics with physical motion.

The Einstein Relation of Kinetic Theory, specifically the Stokes-Einstein Equation, allows us to relate the statistical average displacement, the Diffusion Coefficient, with Boltzmann's Constant [vi], as shown in **Equation 2.**

$$D = \frac{k_B T}{6\pi \eta r}$$ (Equation 2)

Refractive Index

Upon encountering a sudden change in a medium's properties, waves reflect. This reflection may be composed of transverse and longitudinal components. The behavior of these reflections and components is described by Snell's law, which relates angle of incidence and refraction for a wave at a boundary, per **Equation 3**.

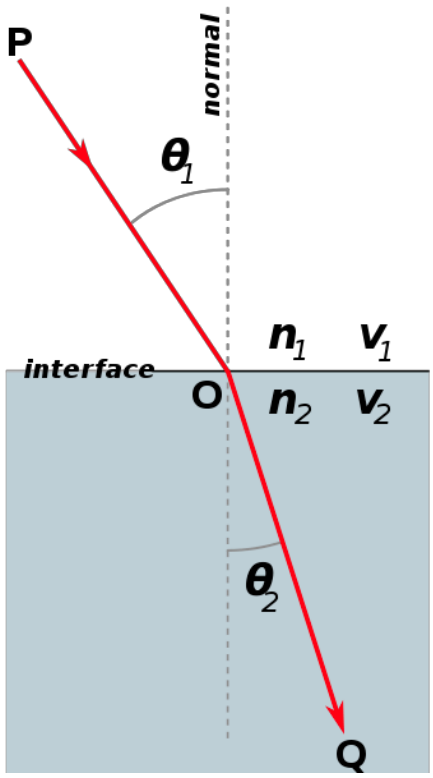

Figure 1: Snell's Law[vii]

$$n_1 \sin\theta_1 = n_2 \sin\theta_2,$$ (Equation 3)

In **Equation 3,** n_1 and n_2 are the indices of refraction, Θ_1 and Θ_2 are the angles form the normal of

the incident and refracted wave, respectively as diagrammed in **Figure 1**.

The behavior of waves at boundaries derives from LaGrangian mechanics, which calculates the probable path as a function of kinetic and potential energy. For light specifically, this related as Fermat's Principle.[viii] Hence, the motion described by Snell's Law is an optimization for minimum energy transversal of a boundary. [ix]

Dielectrics

An insulator that may be polarized with an electric field is a dielectric.[x] The non-conducting object thus forms an electric dipole as charges distribute themselves in the object. When a beam with an electrical gradient is applied to a dielectric, the interaction between the dipole and the dielectric create a force.

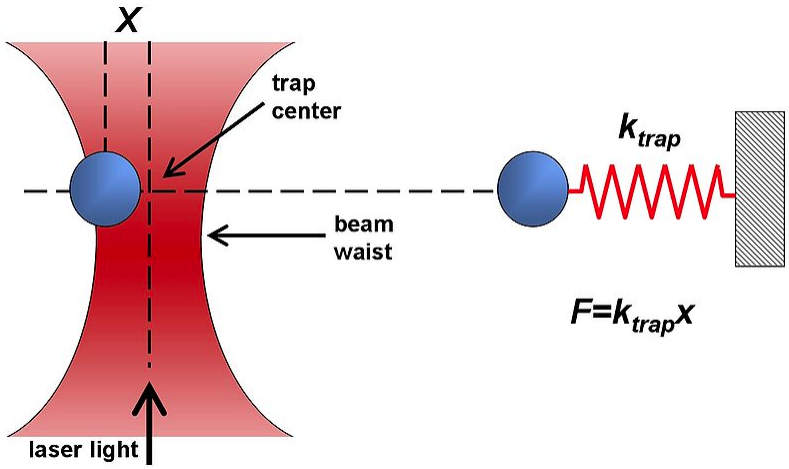

Figure 2: Optical Trapping with Spring Model

Optical Tweezers

Optical tweezers use optics to create a force on dielectric objects.[xi] A focused beam of light may thus be used to hold a microscopic object in place across three dimensions. The 1997 Nobel Prize in Physics was awarded to Steven Chu, Claude Cohen-Tannoudji, and William D. Phillips for their work on trapping neutral atoms.[xii]

Objects are able to be trapped due to the presence of an electric gradient that is strongest at the narrowest point of the beam. Thus, a dielectric object with the aforementioned presence of an electric dipole experiences a restoring force to the center of the trap due to the energy level. This restoring force may be approximated as Hookean in models. [xiii] Momentum is conserved through Snell's law. Specifically, the change in momentum of photons diffracted through the change in medium between the surrounding medium and the object provides the force that drives the object to the center of the trap. At the center of the trap, the angle of incidence is zero, hence there is no diffraction, no change in momentum of photons, and no net force.

Figure 2 [xiv] shows a basic optical trap, including its relation to a Hookean spring model. Optical tweezers have become an important tool in varied areas of science due to their ability to study the mechanics and dielectric properties of microscopic objects and even some sub-micron objects. For instance, a team at MIT was able to attach then subsequently optically trap micron beads at the ends of a molecule of DNA, then calculate the Hookean spring constant of a molecule of DNA by manipulating it with the optical traps.[xv]

Microscope

Microscopy is the application of one or more refractive surfaces in order to magnify the view by manipulating photon paths using Snell's law. [xvi] In a basic example, a curved lens is used, and based on the curvature, light takes different paths through the glass due to the changing incident angles at different points on the curved lens.

An important property of microscopes is the focal length, which describes the distance from the lens where light is focused. As

magnification increases, focal distance decreases. Thus, at high magnification, the use of an oil-immersion lens becomes beneficial. The refractive index of oil, relative to air, allows for a shorter focal length.

The purpose of this experiment is to understand optical tweezers and their use in isolating particles, as well as to characterize Brownian motion in two dimensions by observing through a microscope the motion of the beads and quantifying their movement.

Methods / Procedure

Using an optical tweezers setup based upon that of Bechhoefer and Wilson [xvii], and shown in **Figure 3,** the experiment used a comparison of deterministic and random motion to evaluate the diffusion coefficient of both 1μm and 3μm beads and Boltzmann's constant. 1μm beads were selected on the basis of the Einstein-Stokes equation. Specifically, the proportionality of the radius and the viscosity of the fluid allows quantifiable Brownian motion in the 1um particle, but with the 3um particle the force of gravity becomes quantifiable relative to diffusive effects. The laser trap was used to quantify the motion of the beads within a liquid medium.

Diffusion Coefficient of Small Polystyrene Beads

A buffer solution was prepared using the buffer solution recipe [xviii] and 1μm Polyspherex Polystyrene Microspheres, a slide was made and sealed with Maxi-Cure

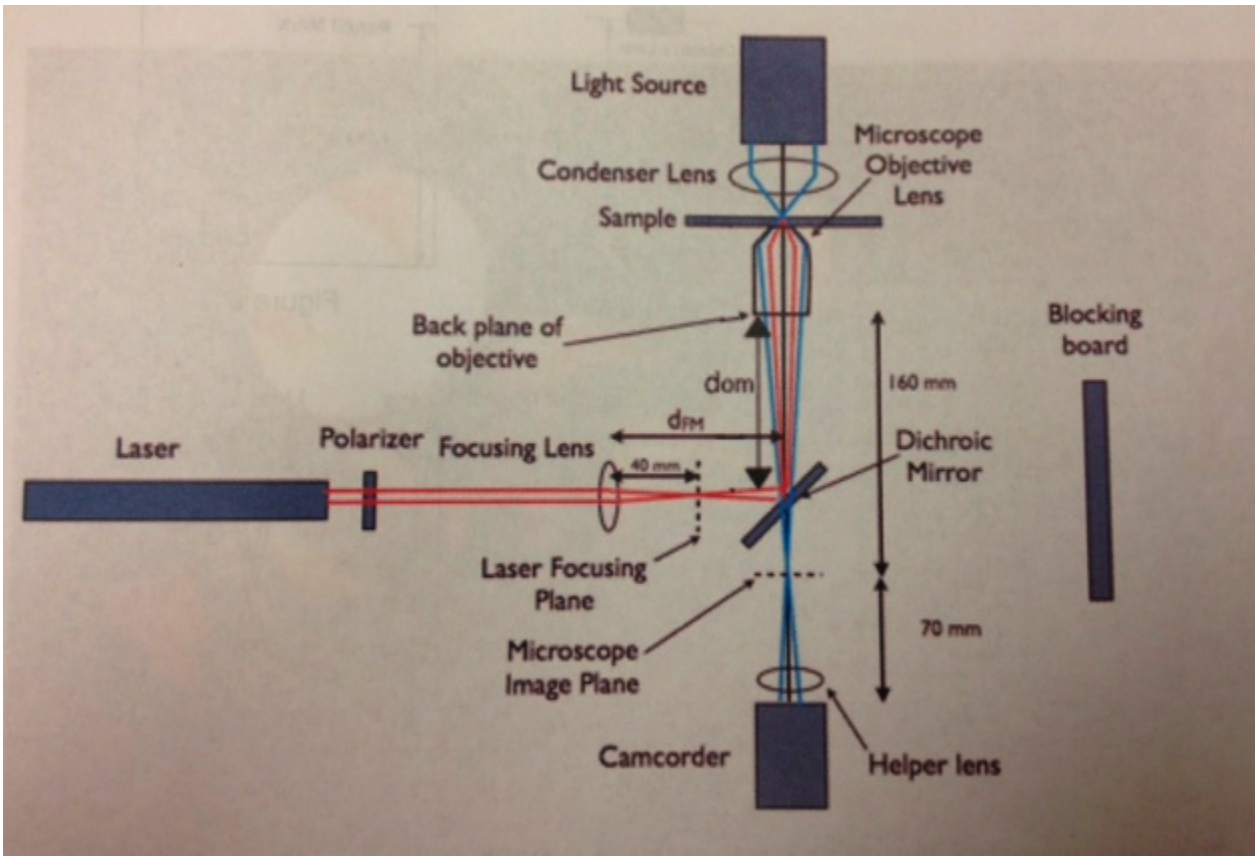

Figure 3: Apparatus Diagram

superglue, hardened with Insta-Set. The buffer was designed to minimize clumping of polystyrene beads in the medium. **Figure 4** demonstrates the construction of a slide. After adding oil to the top of the coverslip due to the use of an oil-immersion objective, the slide was placed in the sample holder. The objective lens was then set closer to the sample holder to be touching the oil on the slide.

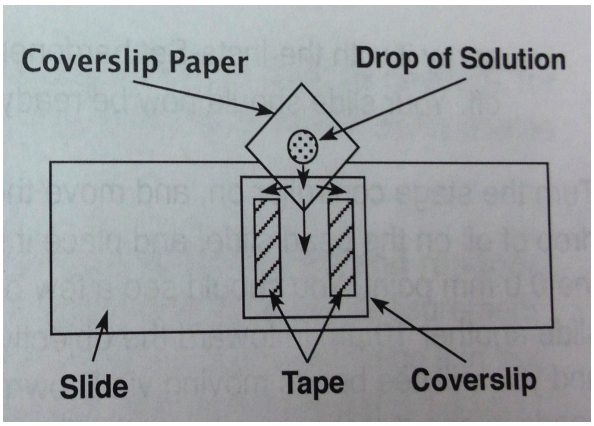

Figure 4: Slide Construction

With the camera set level with the dichroic mirror and the center of the microscope objective lens, facing towards the light source, the camera zoom was adjusted until the beads were visible on an external monitor. The dichroic mirror filters light based on the wavelength. Specifically, light at the laser's wavelength of 632 nm is reflected, while higher wavelengths are able to pass through the lens. This allows the camera to be aligned with the path of the laser as it enters the objective. The focus was then adjusted by moving the objective lens using the control on the stage controller.

Once the beads were focused on the monitor, two minutes of footage was taken using the digital camera. To allow for the conversion of pixel measurements to measurements in meters, the height of the field of view was determined by locating a bead at the top of the screen, recording the y location from the stage controller, moving the stage until the bead was at the bottom of the field of view and then recording the second y location. This physical distance could then be correlated to the field height in pixels.

The video was imported using video manipulation software, and was then cut into 10-second slices. This was done given the limit on the computer's memory. During each step, care was taken to maintain the frame rate and video resolution. Each slice was then converted to 8-bit greyscale and opened individually in ImageJ[xix], a video-processing platform that breaks videos down into static frames and allows photo manipulation on a per-frame basis. Greyscale was chosen because color was not a necessary data point in our analysis, and because converting videos to greyscale lowered memory usage while editing. The program was used to quantify the random motion of the beads by measuring the change in the pixel location of the beads as a function of time, determined from the change in the number of frames.

For each video clip, at least one bead was identified that was in focus and its position was recorded as a pixel coordinate. The clip was then advanced 50 frames, at a known frame rate of 30 frames per second, and the pixel location of the bead center was again recorded as a pixel coordinate. This process was repeated for the duration of the clip, but was ended early if the bead went out of focus or the bead left the frame. The same steps were taken for beads in each of the clip slices until data was obtained for 100 changes in position for beads over 50-frame intervals.

Using the measurement of the number of pixels per distance in millimeters, each set of pixel coordinates was converted to a set of physical coordinates. Changes in position were calculated by subtracting x and y coordinate positions of the bead in one frame from the x and y coordinates of the bead 50 frames later. With knowledge of a frame rate of 30 frames per second and advancement of 50 frames between measurements, the diffusion coefficient (D) was determined using **Equation 4**, where Δx was the change in x position of the bead, Δy was the change in y position of the bead and Δt was the change in time between measurements.

$$D=<\Delta x^2 + \Delta y^2>/(4\Delta t) \quad \text{(Equation 4)}$$

A theoretical prediction was generated from the Einstein-Stokes equation (**Equation 5)**, where k_B was the scientifically accepted value for Boltzmann's constant, T was the air temperature of the room, η was the dynamic viscosity of water[xx], and R was the radius of the bead size given on the Product Data Sheet.

$$D= k_BT/(6\pi\eta R) \quad \text{(Equation 5)}$$

Data for the 3μm bead trials was obtained automatically on a frame-by-frame basis by using the Multitracker plug-in procedure outlined in the lab manual. This procedure computationally returned the pixel coordinates for a selected bead during each frame of the entire clip.

Evaluation of Boltzmann's constant

Using a similar procedure as for the 1μm beads, the motion of 3μm beads provided data for the evaluation of Boltzmann's constant. Instead of using the manual location of the beads within each frame of the clips taken, the Multitracker plug-in for ImageJ was again utilized. The average velocity of the beads in the y direction was determined from the displacement of each bead over a set time period, in this case, one frame. Again, care was taken to ensure that the footage maintained a frame rate of 30 frames per second. The net force (F_{net}) on the bead was calculated from Equation 6, where ρ_{bead} was the density of the bead from the Polymer Data Sheet and ρ_{water} was the density of water.

$$F_{net} = (\text{Bead Volume}) \times (\rho_{bead} - \rho_{water}) \times (\text{acceleration of gravity}) \quad \text{(Equation 6)}$$

The drag coefficient (C_d) was calculated by dividing the net force on each bead by the velocity of the bead. The diffusion coefficient was calculated using only motion in the x direction. Therefore, **Equation 4** leads to **Equation 7**.

$$D=<\Delta x^2>/(2\Delta t) \quad \text{(Equation 7)}$$

The Einstein relation was used to calculate the Boltzmann constant for 3μm beads (Equation 8).

$$D = k_BT / C_d \quad \text{(Equation 8)}$$

With the introduction of the laser, the second dichroic mirror the polarizer and a focusing lens, a trap was created , as shown in Figure 1. Again using the properties of the dichroic mirror, the view of

the laser in the objective was filtered based on its wavelength, thus allowing for unobstructed video capture of the trapped bead.

Laser Trapping

Slides of both stationary and mobile 3μm beads were observed in the presence of the laser trap. Since the beads were able to move in three dimensions and therefore towards and away from the objective lens, the microscope was focused at the depth of each bead targeted. The chosen beads were brought close to the focus of the laser and observed to determine whether the beads were drawn into the trap. Once a bead was trapped, the slide was slowly moved to determine whether the trap was strong enough to control the position of the bead as it travelled through the buffer solution.

Human Blood Cell Trapping

A donor's finger was cleaned with an alcohol wipe and pricked using a 20G 1½ Precision Glide, sterile needle. Two drops of blood were mixed with 1ml of the buffer solution used previously. A coverslip was cut to ⅔ of its original side and two slivers of tape were placed along two opposite edges. The coverslip was then stuck to a clean slide and a piece of the coverslip paper was placed between the coverslip and the slide. Two drops of the blood-buffer solution were injected onto the paper and allowed to permeate under the coverslip. Once the entire area under the coverslip was covered with solution, the paper was removed and the edge of the coverslip was glued and hardened as before.

A drop of oil was placed on the face of the slide and it was then mounted so that its contents could be observed with the objective lens. Blood cells were observed on the slide and exposed to the laser. A video both with and without the dichroic mirror showed how the motion of the cells changed in the presence or absence of the laser.

Results

Diffusion Coefficient of Polystyrene Beads

Based upon the changes in position, velocities and diffusion coefficients found for each 1μm bead during each frame, average values over the entirety of the clip slices were calculated. **Table 1** shows these values along with the standard deviations based upon both manual and Multitracker ascertainment of the beads' positions.

	<Δx> (nm)	**<Δy> (nm)**	**$<V_x>$ (nm/s)**	**$<V_y>$ (nm/s)**	**<D> (nm^2/s)**
Manual	43.352 *(638.140)*	60,939 *(567.640)*	25.510 *(379.165)*	35.860 *(337.299)*	1.09×10^5 *(2.88×10^5)*
Multitracker	-0.848 *(124.046)*	0.166 *(92.200)*	-25.431 *(3721.384)*	4.982 *(2765.990)*	1.79×10^5 *(0.0602)*

Table 1: Motion of 1μm beads (σ in parenthesis)

Based upon the changes in position, velocities and diffusion coefficients in the x direction found for each bead during each frame, average values over the entirety of the clip slices were calculated. **Table 2** shows these values along with the standard deviations.

Bead	**<Δx> (nm)**	**<Δy> (nm)**	**$<V_x>$ (nm/s)**	**$<V_y>$ (nm/s)**	**<D> (nm^2/s)**
3μm Trial 1 Slice 1	-0.723 *(154.175)*	9.481 *(171.565)*	-21.682 *(4625.243)*	-284.425 *(5146.943)*	355382.956 *(566260.431)*
3μm Trial 1 Slice 2	6.951 *(148.835)*	0.909 *(172.273)*	208.542 *(4465.035)*	27.274 *(5168.176)*	331866.426 *(486328.761)*
3μm Trial 1 Slice 3	-12.598 *(159.000)*	30.135 *(186.492)*	-377.952 *(4769.869)*	904.049 *(5594.769)*	379802.962 *(697916,109)*
3μm Trial 1 Slice 4	-11.422 *(176.178)*	-3.777 *(197.546)*	-342.647 *(5285.349)*	-113.317 *(5926.382)*	465422.423 *(704089.122)*
3μm Trial 2	-2.213 *(170.441)*	7.542 *(198.806)*	-66.396 *(5113.228)*	226.282 *(5964.194)*	435435.747 *(924143.075)*

Table 1: Motion of 3μm beads (σ in parenthesis)

Evaluation of Boltzmann's Constant

The average diffusion coefficient in the x direction for each trial was weighted based upon the number of frames in the clip from which the diffusion coefficient was calculated, as shown in **Table 2**. For example, Trial 1 Slice 1 consisted of 305 frames out of the 2155 total frames analyzed. Therefore, the diffusion coefficient counted for approximately 14 percent (305/2155) of the weighted diffusion coefficient.

	Frames	<Δx> (nm)	<Δy> (nm)	σ_x	σ_y	<V_x>(nm/s)	<V_y> (nm/s)	<D_x> (nm^2/s)
Trial 1 Slice 1	305	-0.723	-9.481	154.175	171.565	-21.682	-284.425	355382.956
Trial 1 Slice 2	294	-11.422	0.909	148.835	172.273	208.542	27.274	331866.426
Trial 1 Slice 3	215	-12.598	30.135	158.996	186.492	-377.951	904.049	379802.962
Trial Slice 4	221	-11.422	-3.777	176.178	197.546	-342.648	-113.318	465422.422
Trial 2	1120	-2.213	7.543	170.441	198.806	-66.396	226.282	435435.747
Weighted						-81.972	159.643	407500.955

Table 2: Weighted average of diffusion of 3μm beads

The weighted diffusion coefficient was used in the calculation of Boltzmann's constant, based upon the data shown in **Table 3.**

Diameter (um)	3
Bead Density (g/ml)	1.06
Water Density (g/ml)	1
F_{net} (Newtons)	8.31265×10^{-15}
C_d (kg/s)	5.207×10^{-08}
T (Kelvin)	296.75
Calculated k_B ($m^2kg/(s^2K)$)	7.15032×10^{-23}
Accepted k_B ($m^2kg/(s^2K)$)	1.38065×10^{-23}

Table 3: Calculation of Boltzmann's Constant

Trapped Bead

Table 4 shows the differences in average velocities in both the x and y directions as well as the diffusion coefficient in the x direction as compared between a trapped and an untrapped 3μm bead.

Bead	<Δx> (nm)	<Δy> (nm)	<V_x> (nm/s)	<V_y> (nm/s)	<D_x> (nm^2/s)
Trapped 3μm (11/29)	-0.422 *(52.526)*	0.167 *(45.540)*	12.672 *(1575.791)*	5.025 *(1366.208)*	36181.706 *(39518.143)*
Untrapped 3μm			-81.972	159.643	407500.955

Table 4: Comparison of trapped and untrapped bad motion

Blood Cell Trapping

A comparison of the characteristics of the motion of a trapped and an untrapped blood cell are shown in **Table 5**.

Blood Cell	<Δx> (nm)	<Δy> (nm)	<V_x> (nm/s)	<V_y> (nm/s)	<D_x> (nm^2/s)
Untrapped	6.561 *(286.506)*	-9.067 *(102.534)*	196.849 *(8595.179)*	-271.996 *(3076.018)*	692573.016 *(600742.000)*
Trapped	-3.108 *(195.326)*	-1.816 *(237.911)*	-93.229 *(5859.788)*	-54.492 *(7137.333)*	708872.453 *(655987.790)*

Table 5: Comparison of trapped and untrapped blood cell.

Discussion

Brownian Motion

The results clearly show that observations of the 1μm bead are likely Brownian. This is due to the non-deterministic motion, small displacements, and high standard deviations of the numbers.

Diffusion Coefficient of Polystyrene Bead

The respective diffusion coefficients calculated for the 1μm and 3μm beads show that the effects of gravity were negligible for the 1μm bead when comparing its average x and y displacement. In the 3μm bead, the quantifiable increase in average y displacement relative to average x displacement means that gravity may be reasonably assumed as the introduced force, compared to the 1μm bead.

Boltzmann's Constant

Our calculation of Boltzmann's constant is surprisingly accurate at 317% greater than the accepted value. However, the precision was low based on the high standard deviations of the data.

Increasing the precision of our answer request two things. First, more data will decrease error margins. Second, a major source of error is the radius of the beads. Understanding the manufacturing tolerances of the beads will give a better understanding of the precision of the calculation.

Finally, the most precise way to calculate Boltzmann's constant based on available resources would be with a macroscopic system. Calculating the gas constant based on relating pressure, volume, and temperature of a known molar quantity of gas would give us the quantity equal to Boltzmann's constant times Avogadro's number.

Optical Trapping

Limited experimental success was achieved due to difficulties in obtaining a proper alignment. This limited available data for optically-trapped beads. In addition, difficulty was encountered with identifying a correct bead dilution. An overly-concentrated bead solution caused the aggregation of multiple beads in a single trap. We observed as many as seven beads being held by a single trap. This data was unusable for a quantification of bead movement due the presence of external forces.

However, data shows that trapping was achieved in some capacity for the 3um bead and blood cell. Further experimentation is required to determine the strength of the optical trap. Specifically, moving the bead with the trap may be used to determine the theoretical spring constant of the trap.

Biological applications

Our results show limited success in capturing a blood cell based. This is because, while average displacement decreased under trapping, the data lacks the precision to assert that the change is relevant.

In the future, obtaining more data to increase the precision of these readings could prove more conclusively that the cell was trapped. In addition, conducting experiments based on moving the trapped cell to demonstrate the Hookean nature of an optical trap would be beneficial to quantifying the force on the bead.

Further research could also be done by binding polystyrene beads to the cell membranes of blood cells, thus allowing mechanical properties of the membrane to be determined. In addition, attempts to trap cell organelles could allow for study of the viscosity and movement of the structures in the cell. Specifically, studies of these organelles during mitosis could further understanding of the event based on the ability to isolate or move organelles during mitotic stages.

Error

Because Multitracker was not used initially and the locations of the centers of the beads were performed manually, discrepancies between the diffusion coefficients calculated compared to actuality can stem from error in the locations.

Alignment was a major source of error. Ensuring that the laser was perfectly aligned to shine through the objective, with its focus lying between the slide and cover slip was a major difficulty.

The diameter of the bead was not known precisely. Specifically, manufacturing tolerances are an unknown and probable cause of error. Therefore, some of the error in the calculation of Boltzmann's constant can be attributed to this discrepancy, since the equation used to calculate the constant includes the drag coefficient, which is based upon the bead's volume.

Because only a few seconds of data were collected for the trapped and untrapped blood cell, the results obtained were imprecise. However, we note that the average delta Y does indicate some effect by gravity that was negated by the trapping - so the cell had gravitational effects between the 1um and 3um beads.

Operator error is a possible factor in the use of Multitracker. Specifically, it was infeasible to check every single frame of a given video to ensure a homogeneous cell shape of reasonable form, thus causing possible error in the identification of an object's boundaries.

The specific type of cell trapped in blood was unknown. Knowledge of its type would provide a better understanding of its properties and shape.

One final significant source of error was that we were working with a three-dimensional system, but were attempting to quantify it in two dimensions. Hence, there was motion in the third dimension that was not accounted for. This caused problems with focus as the bead came in and out of view. In addition, it affected the accuracy of our calculation of Boltzmann's Constant.

References

[i] Brown, Robert, "A brief account of microscopical observations made in the months of June, July and August, 1827, on the particles contained in the pollen of plants; and on the general existence of active molecules in organic and inorganic bodies." Phil. Mag. 4, 161–173, 1828.

[ii] Marshall, T. W. (2000). Brownian motion, the second law and Boltzmann.*European Journal of Physics*, *3*(4), 215. doi:10.1088/0143-0807/3/4/005

[iii]Pearson, K. (1905). The Problem of the Random Walk. Nature. 72, 294.

[iv]Reif, F. (1964). Fundamentals of Statistical and Thermal Physics. ISBN 1577666127.

[v] Berg, Howard C. (1993). *Random Walks in Biology.* ISBN: 0691000646.

[vi] Edward, John T. (1970) Molecular volumes and the Stokes-Einstein equation. Journal of Journal of Chemical Education 1970 47 (4), 261

[vii]http://en.wikipedia.org/wiki/File:Snells_law2.svg (Public Domain)

[viii] Feynman, Richard. The Feynman Lectures on Physics, Vol. 1. pp. 26–7.

[ix] Weisstein, Eric W. "Snell's Law." *Snell's Law -- from Eric Weisstein's World of Physics*. Wolfram Research, 2007. Web. 23 Oct. 2012. <http://scienceworld.wolfram.com/physics/SnellsLaw.html>.

[x] David J. Griffiths. Introduction to Electrodynamics (3rd Edition). Benjamin Cummings, 1998.

[xi] http://www.bell-labs.com/user/feature/archives/ashkin/

[xii] http://www.nobelprize.org/nobel_prizes/physics/laureates/1997/

[xiii] Neuman, Keir C., and Attila Nagy. "Single-molecule force spectroscopy: optical tweezers, magnetic tweezers and atomic force microscopy." *Nature methods*5.6 (2008): 491-505.

[xiv] http://en.wikipedia.org/wiki/File:Optical_Trap_As_a_Spring.jpg

[xv] http://web.mit.edu/cepstein/Public/CEpsteinDNA.pdf

[xvi] Feynman, Richard. The Feynman Lectures on Physics, Vol. 1. Chapter 27

[xvii] Bechhoefer, J. and Wilson, S. (2002). Am. J. Phys. 70, 393-400.

[xviii] Physics 360 Optical Tweezers Lab Manual, 25 Aug. 2012.

[xix] ImageJ: Image Processing and Analysis in Java. Web. 13 Nov. 2012. <http://rsb.info.nih.gov/ij>.

[xx] "Dynamic and Kinematic Viscosity of Water in Imperial Units (BG Units)." The Engineering Toolbox. Web. 8 Nov. 2012. <www.engineeringtoolbox.com>.